Eric Jonsson School of Engineering and Computer Science

2001-6

Chromatic Dispersion and Self-Phase Modulation in Multi-Hop Multi-Rate WDM Rings

Isabella Cerutti, *et al.*

Chromatic Dispersion and Self-Phase Modulation in Multi-Hop Multi-Rate WDM Rings

Isabella Cerutti, Andrea Fumagalli, Mary J. Potasek

Technical Report UTD/EE/01/2001
June 2001

Chromatic Dispersion and Self-Phase Modulation in Multi-Hop Multi-Rate WDM Rings *

Isabella Cerutti⋆, Andrea Fumagalli⋆, Mary J. Potasek◇

⋆ Optical Networking Advanced Research (OpNeAR) Lab
University of Texas at Dallas, Richardson, TX 75080.
E-mails: {isabella, andreaf}@utdallas.edu

◇ Courant Institute, New York University, New York, NY
E-mail: mpotasek@aol.com

Abstract

When compared to first generation and single-hop optical networks, multi-hop and multi-rate (M&M) network architectures have the advantage of significantly reducing network design cost under a variety of wavelength-to-terminal cost ratios. This report investigates how fiber chromatic dispersion and self-phase modulation may affect such cost reduction in M&M WDM rings.

Keywords: Chromatic dispersion, self-phase modulation, network design, multi-hop, multi-rate network.

1 Introduction

Propagation of the optical signals through fibers and optical nodes — the so called *transparency* of optical networks — provides the network designers with a number of alternative network architectures to choose from [1, 2], e.g., wavelength routing, broadcast-and-select, and photonic slot routing networks. The common objective of these architectures is to eliminate, or significantly reduce, the relatively slow and cumbersome electronic processing of the transmitted signal at the intermediate nodes.

Among these architectures, wavelength routing networks make use of Wavelength Division Multiplexing (WDM) to create multiple coarse-bandwidth channels (i.e., wavelengths) in the fiber. To efficiently exploit each wavelength bandwidth, traffic grooming is thus required. It is important to observe that with current technology traffic grooming is possible only using electronics. Three classes of traffic grooming solutions are briefly summarized.

In conventional First Generation (FG) optical networks, i.e., SONET/SDH, traffic grooming is performed at each intermediate node, thus potentially achieving bandwidth-efficient solutions at the cost of a large number of Optical Terminals (OT).

In Single-Hop (SH) optical networks, less OTs are used as they are required only at the end nodes of the optical circuit or lightpath [3]. Once transmitted, the optical signal propagates along the lightpath without requiring O/E and E/O conversion, until it is received at the destination

*The work was partially supported by the Texas Higher Education Coordinating Board under contract # 009741-0139-1999, TxTEC, and NSF under contract # ANI-0082085.

node. Grooming is limited among the tributary signals that share the same source-destination pair.

A generalization of both FG and SH network architectures is the Multi-hop and Multi-rate (M&M) [4] architecture in which the tributary signal is transmitted from source to destination through multiple lightpaths, or optical hops, and the transmission rate of each hop may differ from one another. Multi-hop transmission yields reduced number of OTs (and associated electronics) when compared to FG architecture and reduced number of wavelengths when compared to SH architecture. In addition, the multi-rate feature provides the network designer with the flexibility of selecting the most cost effective OT on a per-lightpath basis, as opposed to single-rate solutions in which all lightpaths must be transmited at the same rate. It has been shown that in a WDM ring, the M&M architecture has the potential to yield significant cost reductions when compared to FG and SH rings [4].

The results presented in [4] are obtained under the assumption that the behavior of the optical medium is close to ideal, i.e., transmission impairments do not limit the transparency of the optical signal. However, in certain instances, transmission impairments induced by available fibers and optical components, may significantly restrain the signal transparency and must be taken into account during the network design.

For example, chromatic dispersion — also known as Group Velocity Dispersion (GVD) — causes different spectral components of the optical pulse to travel at slightly different group velocities. GVD causes pulse broadening that is detrimental to optical systems and thus may limit the maximum pulse propagation distance. A number of nonlinear effects [5] — originating from the dependence of the refractive index on the intensity of the transmitted light — may also induce signal distortion. At low bit rates, i.e., 2.5 Gb/s and below, these impairments may not significantly affect optical transmission, especially over relatively short distances. However, as the channel bit rate increases to 10 Gb/s and beyond, some of these nonlinear effects, combined with chromatic dispersion, may degrade the signal considerably. Among the nonlinear effects, Self-Phase Modulation (SPM) plays an important role in optical transmission systems [6, 7]. SPM originates from the fact that the nonlinear index of refraction causes an induced phase shift proportional to the intensity of the pulse. Therefore, different parts of the pulse experience different phase shifts resulting in a chirping of the pulse. This SPM-induced chirp interacts with the pulse broadening effects caused by dispersion and may further limit the channel bandwidth-distance product.

In the presence of the above undesirable effects the quality of the optical signal may degrade significantly and, practically speaking, the maximum span of a lightpath may be constrained. In other words, the transparency degree of the network may be limited if no countermeasures are taken to compensate for such signal degradation.

The goal of this report is to assess the impact of both GVD and SPM on the overall design and cost of FG, SH, and M&M networks. The study is based on the assumption that efficient optimization algorithms, that ultimately determine the span and rate of each lightpath, are combined with an analytical expression that estimates the signal degradation due to both GVD and SPM. The study is carried out using a SONET-over-WDM ring benchmark. Numerical results obtained using the ring benchmark are shown that reveal how the transmission limitations induced by GVD and SPM may affect the overall optimal network design and cost. Based on the presented results, it is possible to determine whether compensation of dispersion and self-phase modulation may yield a significant cost reduction of the SONET-over-WDM ring.

2 SONET-over-WDM Ring Architectures

In its broadest definition, each node of a SONET-over-WDM ring consists of an Optical Add-Drop Multiplexer (OADM) that demultiplexes (multiplexes) the incoming (outgoing) wavelengths and provides each wavelength with either optically transparent by-pass transmission or add-drop termination of the lightpath. Each dropped (added) wavelength is received (transmitted) by an Optical Terminal (OT) that feeds (is fed by) an electrical Add/Drop Multiplexer (ADM). At the ADM various tributary signals, i.e., STS-1s (51.84 Mb/s), are de-multiplexed and handled individually. Each node in the ring is independently assigned a minimum transmission rate and a maximum transmission rate. These rates are represented, respectively, by the minimum and maximum SONET/SDH OC rates that the node OTs can handle, i.e., available rates are OC-m with $m \in M = \{3, 12, 48, 192, \dots\}$. The transmission rate chosen for a lightpath must be available at both channel's end nodes. Multiple Rates (MR) are thus available and can be assigned to distinct lightpaths.

With the above broad framework, the following three architectures can be modeled:

- FG-MR: lightpaths are all terminated at every node, and the transmission rate is chosen individually for each lightpath;
- SH-MR: tributary signals must span across a single lightpath, i.e., lightpaths are all terminated at the source and destination nodes of their tributary signals only, and the transmission rate is chosen individually for each lightpath; and
- M&M: tributary signals may span across multiple lightpaths, and the transmission rate is chosen individually for each lightpath.

Once the preferred architecture is chosen, the problem that remains to be solved is the selection of the lightpaths required to carry the offered traffic. For each lightpath, the span and the transmission rate must be determined, keeping in mind that GVD and SPM may practically limit the lightpath maximum distance-bandwidth product. As discussed next, the optimal choice of the lightpath set is not always a trivial problem.

2.1 GVD- and SPM-Constrained Design

As already mentioned, GVD causes different spectral components of the optical pulse to travel at slightly different group velocities, thus inducing a temporal broadening of the pulse. SPM broadens the optical pulse spectrum and induces a chirp that interacts with the dispersion-induced chirp. The resulting pulse broadening ratio, K, defined as the ratio between the root mean square (rms) width of a pulse at a distance z and its initial rms width, may be estimated using the approximated analytical expression [8]

$$K = \sqrt{1 + \sqrt{2}\phi\frac{\beta_2 z}{\sigma^2} + \left(1 + \frac{4}{3\sqrt{3}}\phi^2\right)\left(\frac{\beta_2 z}{\sigma^2}\right)^2} \tag{1}$$

where β_2 is the first order dispersion parameter — higher order dispersive effects are considered negligible; σ represents the $1/e$ half-width of the Gaussian pulse intensity and can be approximated by $\sigma = \frac{1}{4B}$ for return to zero (RZ) pulses, with B the lightpath bit rate; ϕ is the maximum intensity-dependent phase shift due to SPM. An expression for ϕ is $\phi = \frac{n_2 \omega_0}{c} A_0^2 z_{eff}$, where n_2 is the nonlinear term of the refraction index; ω_0 is the carrier frequency; c is the velocity of light in vacuum; A_0^2 is the input pulse intensity; and z_{eff} is the effective distance. The effective distance depends on the fiber attenuation constant α as $z_{eff} = (\frac{1-exp(-\alpha z)}{\alpha})$. In absence of fiber loss, $\alpha = 0$ and $z_{eff} \rightarrow z$. The input pulse intensity, ${A_0}^2 = \frac{P}{A_{eff}}$, is proportional to the peak power, P, and to the effective cross sectional area of the fiber core, A_{eff}. If the fiber is considered as a linear medium, then $n_2 = 0 \rightarrow \phi = 0$. Equation 1 is fairly accurate for values of $\phi < 1$ [8]. In order to ensure a desired K, Equation 1 may be used to pose a limit on the maximum pulse propagation distance.

In absence of fiber loss, i.e., $\alpha = 0$, the allowed maximum lightpath length, L_{max}, assuming an acceptable broadening factor K, can be expressed analytically as:

$$L_{max} = \left\{ \frac{-3\sqrt{3}}{8\phi_c^2 \cdot \frac{\beta_2}{\sigma^2}} \cdot \left[\sqrt{2}\phi_c + \frac{\beta_2}{\sigma^2} + \left(2{\phi_c}^2 (1 - \frac{8}{3\sqrt{3}} \cdot (1-K^2)) + \frac{{\beta_2}^2}{\sigma^4} + 2\sqrt{2}\phi_c \cdot \frac{\beta_2}{\sigma^2} \right)^{\frac{1}{2}} \right] \right\}^{\frac{1}{2}} \qquad (2)$$

where $\phi_c = \frac{n_2 \omega_0}{c} A_0^2$. As demonstrated in [7, 9], $\alpha = 0$ can be assimilated to the case of compensation of the fiber loss with periodically spaced optical amplifiers. In this case power P is interpreted as the average over the amplifier spacing L_a

$$P = \frac{1 - e^{-\alpha L_a}}{\alpha L_a} P_a \qquad (3)$$

where P_a is the amplifier output power.

In the presence of fiber loss, solving Equation 1 for L_{max} requires the use of numerical methods, such as the bisection method.

2.1.1 Optimal Design in the Presence of Non Ideal Medium

Since Equation 1 may practically restrict the allowed lightpath bandwidth-distance product, the set of lightpaths that can be chosen to design the network may be significantly reduced when compared to the ideal medium case in which any lightpath with any rate is permitted. Restricting the set of lightpaths available to design the SONET-over-WDM ring, may have a significant impact on the optimal design and overall cost of the FG-MR, SH-MR, and M&M architectures.

Consider for example the case in which the network cost is defined as the sum of the wavelength cost (proportional to the total wavelength mileage) and the OT cost (proportional to the number of terminals and their transmission rate). In the presence of ideal medium an optimal design for the FG-MR, SH-MR and M&M network architectures exists which minimizes the overall network cost [4]. In [4] an exact ILP formulation of the optimization problem is provided. For both FG-MR and SH-MR architectures the optimal design is found with the use of optimal algorithms. For the M&M architecture the problem is in general NP-hard. A sub-optimal algorithmic approach is proposed to find efficient solutions in polynomial time.

The problem formulation and solutions discussed in [4] must be modified to take into consideration Equation 2, derived for the non ideal medium case. The following constraint must be added to the problem formulation provided in [4].

Let variable $l^{ij,m}$ denote the number of lightpaths operating at OC-m between node i and j that are required to carry the offered traffic. If the route length between node i and j is longer than the maximum length obtained from Equation 1, then it is necessary to impose $l^{ij,m} = 0$.

3 Cost Comparison of Various SONET-over-WDM Ring Designs

This section presents some numerical results obtained for a six-node unidirectional ring benchmark. Nodes are numbered from 1 to 6, with node 2 the first downstream node from node 1, etc. Line lengths are: $d_{(1,2)} = d_{(2,3)} = 15$ km, $d_{(3,4)} = d_{(4,5)} = 20$ km, and $d_{(5,6)} = d_{(6,1)} = 55$ km. Nodes $1, 3, 5$ transmit and receive at rates from OC-3 up to OC-192. Nodes $2, 4, 6$ transmit and receive at rates from OC-3 up to OC-48. The traffic matrix is complete (with a diagonal of zeros) and uniform with 64 STS-1 tributary signals from any node to any other node. The OT cost, c^m_{OT}, is assumed to double for a 4-fold growth of the working bit rate OC-m, i.e., $c^{4m}_{OT} = 2 \cdot c^m_{OT}$. The wavelength cost, c_w, is assumed to be unitary for each km of wavelength. To explore different cost ratios between the optical bandwidth and OT cost, parameter $\gamma = \frac{c_w \cdot L_{av}}{c^3_{OT} + c_w \cdot L_{av}}$, $\gamma \in (0, 1]$ is defined, where L_{av} is the average line length. Given c_w and γ, it is possible to evaluate c^3_{OT} and consequently c^m_{OT} $\forall m \in M$. When $\gamma \to 0$ the OT cost is dominant. When $\gamma = 1$ the wavelength cost is dominant. Other values represent all possible intermediate wavelength-to-OT cost ratios.

The allowed maximum broadening of the initial pulse is 5%, i.e., $K = 1.05$. Pulses have a carrier frequency in the 1.55 μm region. Unless otherwise specified, the transmitted peak power is $P = 9$dBm, traveling in nonlinear ($n_2 = 2.6 \cdot 10^{-16}$cm^2/W), dispersive ($\beta_2 \in [-20, -2]$ ps^2/km) and attenuated ($\alpha = 0.2$ dB/km) fibers, with $A_{eff} = 47\mu$m^2. The chosen dispersion values cover a representative range of fiber types and possible wavelengths. To emphasize the effect of GVD on the network cost, the presented results focus on the fiber anomalous dispersion region.

Figures 1 and 2 illustrate the lightpath maximum length imposed by GVD and SPM. Figure 1 shows that the lightpath maximum length imposed by SPM and GVD is strongly limited at high transmission rates and significantly decreases as the fiber dispersion factor increases in magnitude, $|\beta_2|$.

The dependence of L_{max} on β_2 and P is graphically shown in Fig 2 for an OC-192 channel. Two surfaces are shown and represent case $\alpha = 0$ dB/km and case $\alpha = 0.2$ dB/km, respectively. In the presence of signal loss ($\alpha = 0.2$ dB/km) the power reduction of the pulse as it propagates along the lightpath reduces the SPM negative impact on the signal quality. As a result, the maximum propagation distance increases up to a maximum value corresponding to an input power of about 20 mW. Except for low values of $|\beta_2|$, the two surfaces do not differ significantly and are more sensitive to variation of β_2 rather than to variation of the peak power.

The impact of GVD and SPM on the (minimum) cost of various ring architectures is illustrated in Figures 3 through 9. The cost of different architectures (FG-MR, SH-MR, and M&M) is plotted using both the optimal design approach devised for the Ideal Medium (IM) [4] and the optimal design approach presented in this report (GVD-SPM), that assumes non-negligible chromatic dispersive (GVD) and self-phase modulation (SPM) fibers (Section 2.1).

Figures 3 and 4 show the impact of a non-ideal medium on the overall network cost for a peak power of $P = 9$ dBm. Figure 3 compares the cost of the M&M architecture to the cost of the FG-MR and SH-MR architectures, in the presence of GVD and SPM. Network cost is

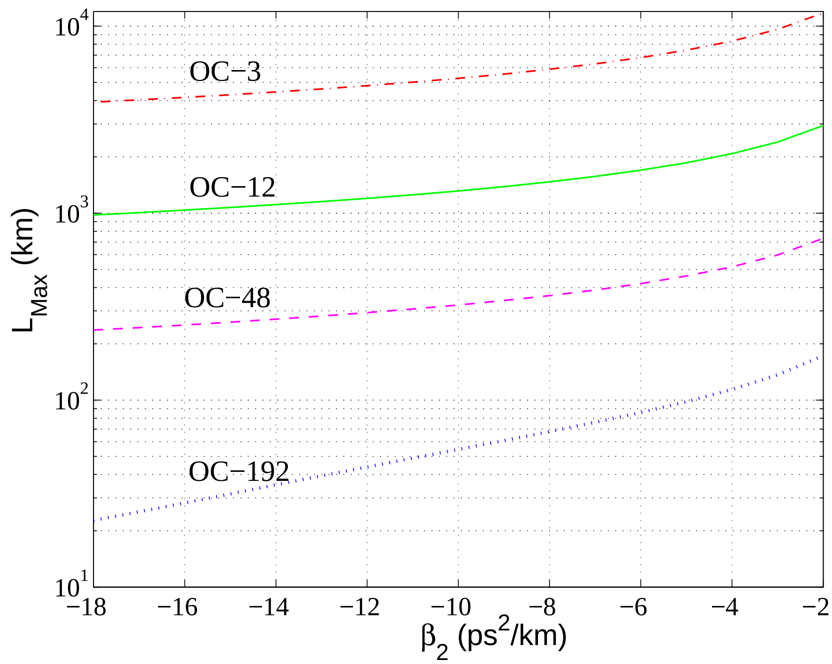

Figure 1: Lightpath maximum distance (Equation 2) versus β_2 for different OC rates

	IM	**GVD - SPM**				
		$\beta_2 = -3$	$\beta_2 = -4$	$\beta_2 = -8$	$\beta_2 = -10$	$\beta_2 = -14$
M&M, $\gamma = 0.05$	(36,3)	(36,3)	(39,2)	(39,2)	(42,1)	(45,0)
M&M, $\gamma = 0.5$	(33,5)	(35,5)	(39,2)	(39,2)	(42,1)	(45,0)
M&M, $\gamma = 0.95$	(33,6)	(33,8)	(41,5)	(41,6)	(44,3)	(45,0)
SH	(48,6)	(52,4)	(54,3)	(56,2)	(58,1)	(60,0)

Table 1: Distribution of lightpaths (OC-48, OC-192) for various architectures when $\alpha = 0.2$ d-B/km

normalized to the M&M-IM cost. In both SH-MR and M&M architectures, large values of $|\beta_2|$ yield increased network cost. Overall, the cost-effectiveness of the M&M architecture still holds, but may be significantly reduced by GVD and SPM. This is due to the fact that GVD and SPM may force the use of multiple lightpaths at lower rate instead of a single lightpath at higher rate between nodes that are far apart from each other. This speculation is confirmed by the results shown in Table 1, whose entries are two-ples indicating, respectively, how many OC-48 and OC-192 lightpaths are required in various solutions. The FG-MR architecture is insensitive to the variation of β_2 in this particular example, because of the relative short line lengths used in the experiment. The cost of the M&M solution obtained in polynomial time using the sub-optimal algorithm is approximately 10% from the optimal solution found using the ILP solver. Notice that the choice of a different fiber (e.g., a different value of β_2) may lead to a different optimal network design.

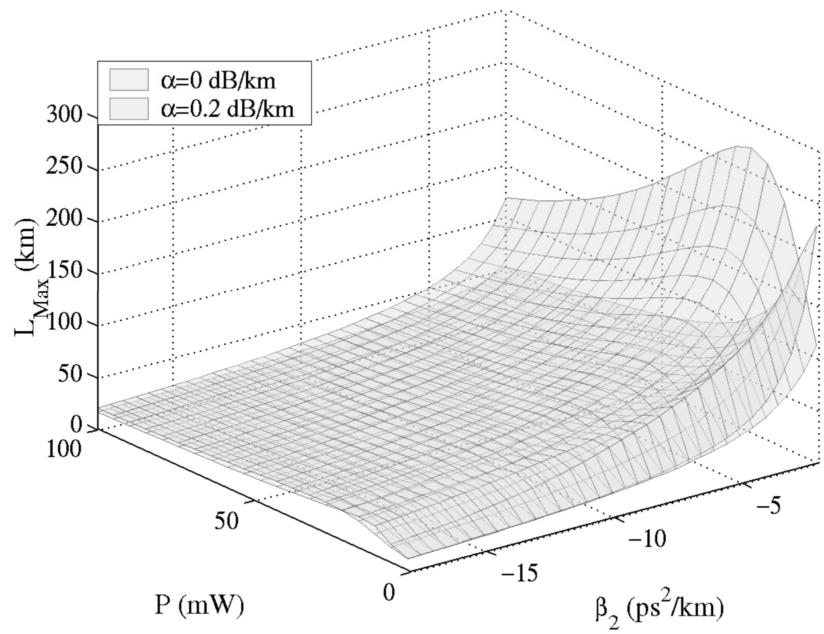

Figure 2: Lightpath maximum distance versus β_2 and P

Figure 5 illustrates the normalized cost of the M&M architecture versus γ for a variety of possible scenarios: $\beta_2 = -3, -10$ ps^2/km, and $P = 6, 9, 12$ dBm. The negative impact of GVD and SPM is more visible at high values of γ, which represent the case of dominant wavelength cost. The total network cost is affected not only by the fiber dispersion (see Figures 3 and 4), but also by the peak power. The cost variation due to P is large at high values of γ and appears to be less sensitive to the variation of peak power at low values of γ, in accordance with Figure 2.

Figures 5, 4, 6, 7 further document the impact of the peak power on the overall network cost.

When fiber attenuation is considered, $\alpha = 0.2$ dB/km, (Figures 7 and 9) high peak power yields better bandwidth-distance product, thus potentially reducing the overall network cost. This fact only marginally affects the total network cost at low values of γ (Figure 9) but it becomes evident at large values of γ (Figure 7).

In the presence of optical amplifiers, $\alpha = 0$ dB/km, (Figures 6 and 8) the choice of the best peak power depends on the fiber dispersion value. High peak power leads to reduced network cost in the presence of highly dispersive fibers. On the other hand, low peak power is preferable in low dispersion fibers, in accordance with the plots shown in Figure 2.

Overall, the optimal selection of the peak power is an important cost factor, especially in M&M architectures. Figures 7 and 9 show that in M&M architectures, the network cost can be reduced by up to 40%, while in SH-MR architectures the network cost can only be reduced by up to 10%.

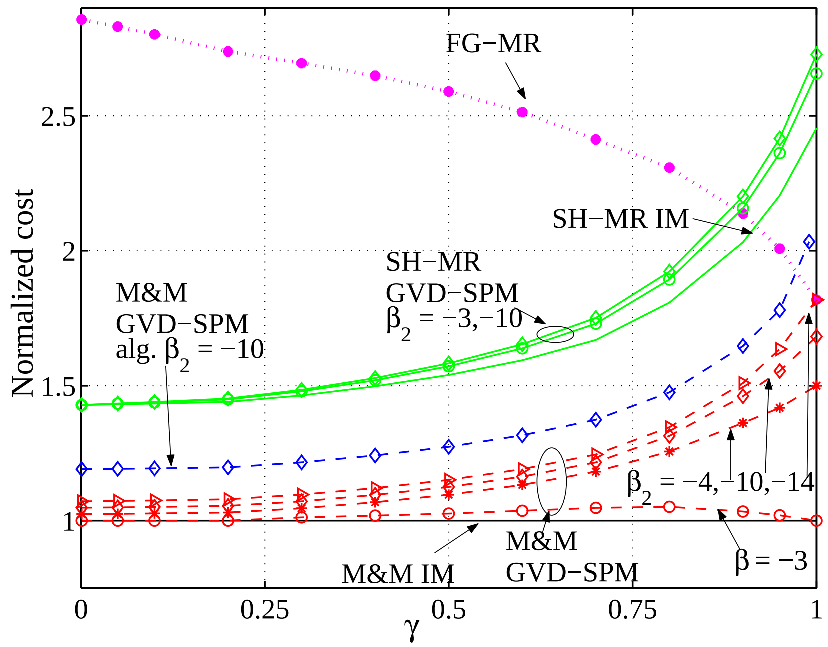

Figure 3: Normalized network cost versus γ, for case $\alpha = 0.2$ dB/km

4 Conclusion

Although restricted to chromatic dispersion and self-phase modulation, this initial study indicates that the conclusions reached with the analysis in Section 3 may be considerably altered when transmission impairments are taken into consideration. Depending on the traffic distribution and network size, the use of dispersion compensation mechanisms in nonlinear dispersive fibers may be advisable, in order to fully benefit from the advantages provided by optical channel transparency.

In conclusion, to fully understand the ultimate potential of optical transparency, especially in designing M&M networks, it is necessary to further study the impact that other transmission impairments — such as polarization mode dispersion, cross-phase modulation, four-wave mixing, and stimulated Raman scattering — may have on the overall network cost optimization problem.

References

[1] R. Ramaswami and K. N. Sivarajan, *Optical Networks: a pratical prospective*, Morgan Kaufmann Publishers, Inc., 1998.

[2] B. Mukherjee, *Optical Communication Networks*, McGraw-Hill, 1997.

[3] I. Chlamtac, A. Ganz, and G. Karmi, "Lightpath communications: a novel approach to high bandwidth optical WAN-s," *IEEE Transactions on Communications*, vol. 40, no. 7, pp. 1171–1182, July 1992.

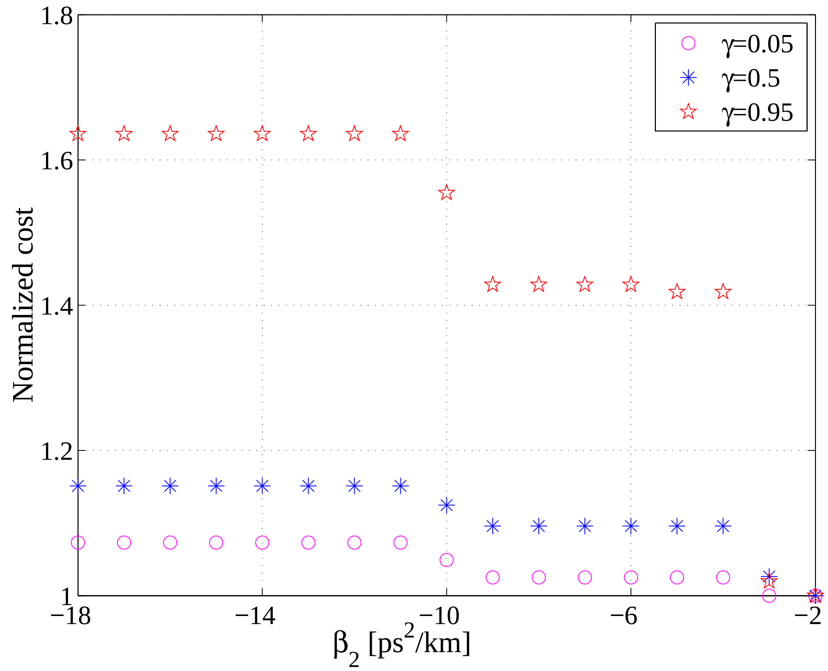

Figure 4: Normalized M&M network cost versus β_2, for case $\alpha = 0.2$ dB/km

[4] I. Cerutti, A. Fumagalli M. Tacca, A. Lardies, and R. Jagannathan, “The Multi-Hop Multi-Rate Wavelength Division Multiplexing ring,” *Journal of Lightwave Technology -special issue on ”Optical Networks”*, vol. 18, no. 12, pp. 1649–1656, December 2000.

[5] G. P. Agrawal, *Nonlinear Fiber Optics*, Academic Press, 2nd edition, 1995.

[6] M. Stern, J. P. Heritage, and R. N. Thurstonand S. Tu, “Self-phase modulation and dispersion in high data rate fiber-optic transmission systems,” *Journal of Lightwave Technology*, vol. 8, no. 7, pp. 1009 –1016, 1990.

[7] A. Naka and S. Saito, “In -line amplifier transmission distance determined by self-phase modulation and group velocity dispersion,” *Journal of Lightwave Technology*, vol. 12, no. 2, pp. 280–287, 1994.

[8] M. J. Potasek, G. P. Agrawal, and S. C. Pinault, “Analytic and numerical study of pulse broadening in nonlinear dispersive optical fibers,” *Journal of Optical Society of America B*, vol. 4, pp. 205–212, 1986.

[9] D. Marcuse, “RMS width of pulses in nonlinear dispersive fibers,” *Journal of Lightwave Technology*, vol. 10, no. 1, pp. 17–21, 1992.

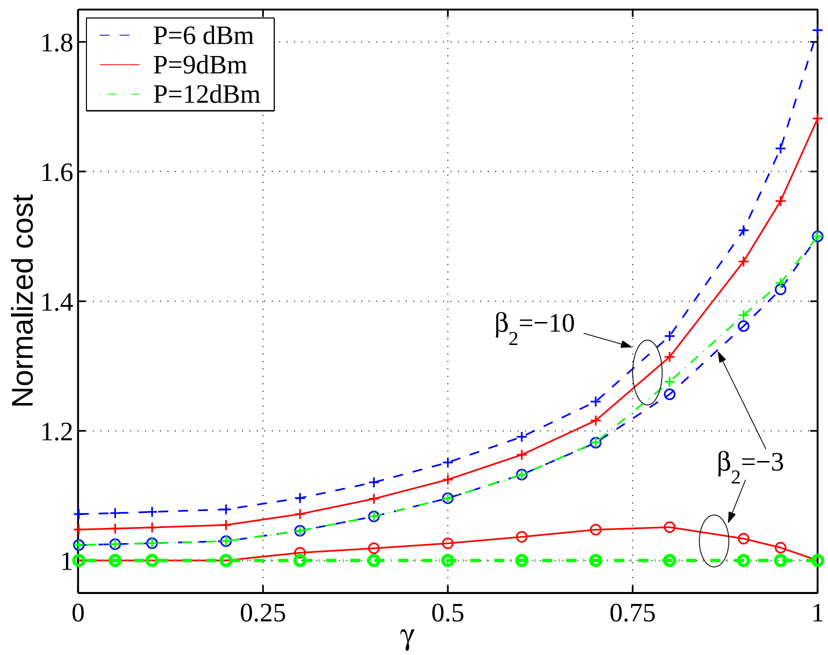

Figure 5: Normalized M&M network cost versus γ, for case $\alpha = 0.2$ dB/km

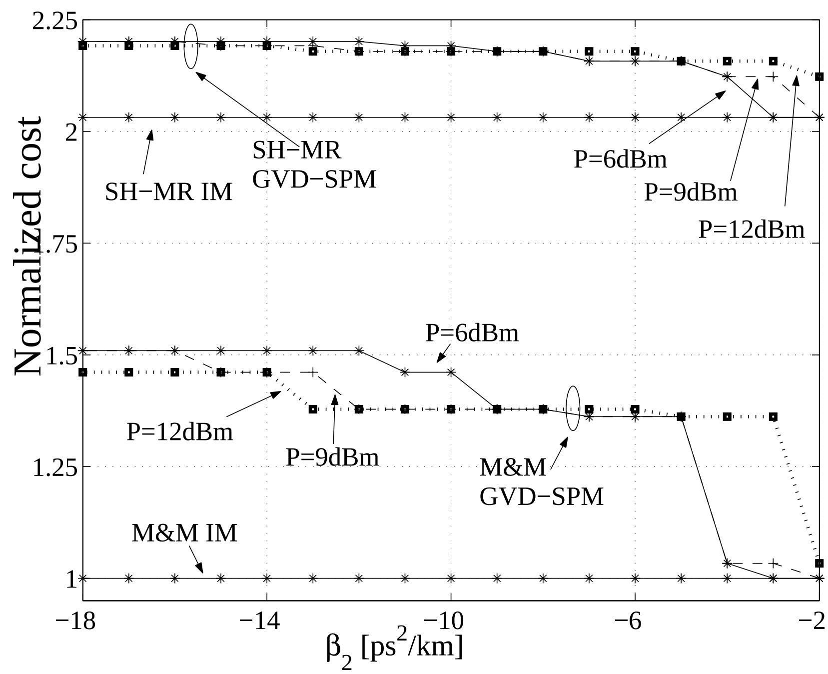

Figure 6: Normalized M&M network cost versus β_2 for different values of peak power, $\alpha = 0$ dB/km, and $\gamma = 0.9$

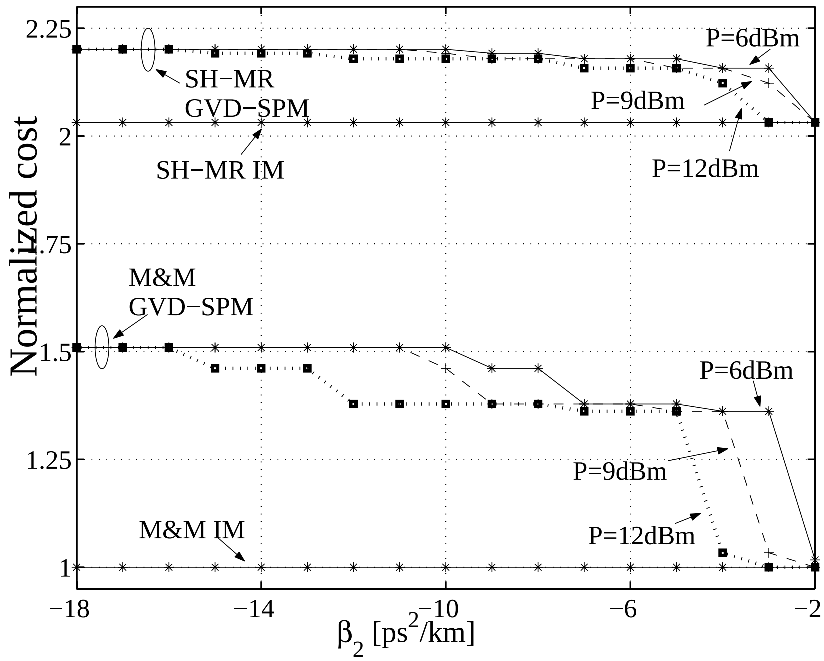

Figure 7: Normalized M&M network cost versus β_2 for different values of peak power, $\alpha = 0.2$ dB/km, and $\gamma = 0.9$

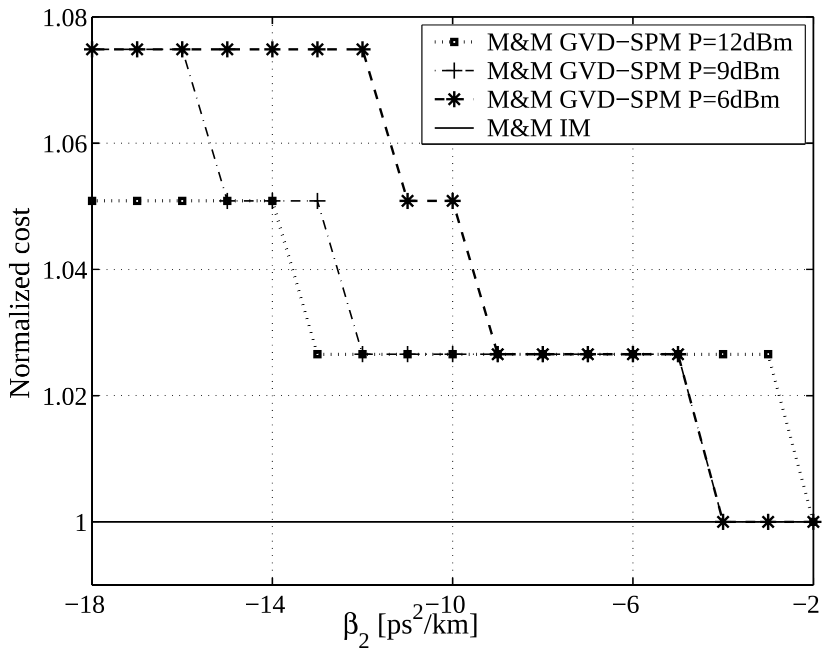

Figure 8: Normalized M&M network cost versus β_2 for different values of peak power, $\alpha = 0$ dB/km, and $\gamma = 0.1$

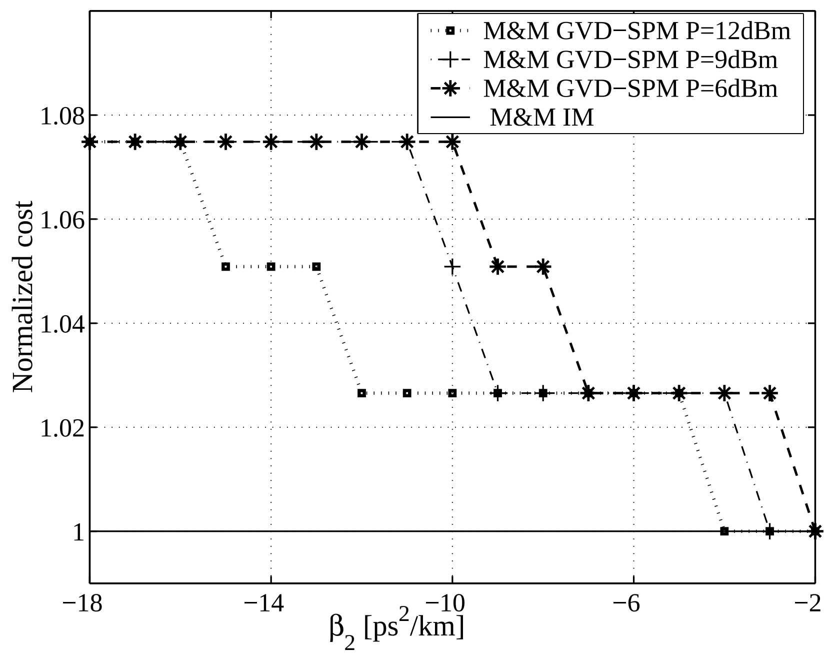

Figure 9: Normalized M&M network cost versus β_2 for different values of peak power, $\alpha =$ 0.2 dB/km, and $\gamma = 0.1$